

# Gamma irradiation effects on Al/n-Si Schottky junction properties

Indudhar Panduranga Vali<sup>a</sup>, Pramoda Kumara Shetty<sup>a,\*</sup>, M.G. Mahesha<sup>a</sup>, Rashmitha Keshav<sup>a</sup>, V.G. Sathe<sup>b</sup>, D.M. Phase<sup>b</sup>, R.J. Choudhary<sup>b</sup>

<sup>a</sup> Department of Physics, Manipal Institute of Technology, Manipal Academy of Higher Education, Manipal 576104, India

<sup>b</sup> UGC-DAE Consortium for Scientific Research, University Campus, Khandwa Road, Indore 452017, India

## ARTICLE INFO

### Keywords:

Gamma irradiation  
Schottky barrier height  
Interface traps  
XPS  
Effective work function

## ABSTRACT

In this paper the gamma irradiation effects on the structural and electrical properties of n-Si and Al/n-Si Schottky junctions are presented up to a cumulative radiation dose of 1500 kGy. The structural studies using XRD and Raman spectroscopic techniques showed no greater degradation in the crystallinity of the n-Si crystals due to the irradiation effects. However, considerable variations in the I–V characteristics of Al/n-Si Schottky junctions and its junction parameters such as Schottky barrier height ( $\Phi_B$ ), ideality factor ( $n$ ) and series resistance ( $R_s$ ) indicates the presence of gamma induced defect states in the interface as well as bulk of the crystal. The surface and interface analysis of the irradiated Al/n-Si Schottky junction revealed modification in the effective work function of Al and presence of different chemical states ( $\text{AlO}_x$ – $\text{SiO}_x$ ) in the interface. The contribution of these interface trap states on the band bending properties and I–V characteristics are explained in detail by realizing the power law characteristics and energy band diagram of the Al/n-Si Schottky junction.

## 1. Introduction

It is well-known that the rectifying metal-semiconductor or Schottky contacts are ideal for microwave, switching, gating and clamping applications in the semiconductor device technology [1,2]. The electrical properties of these Schottky contacts are found to depend on various factors such as work function of metal and semiconductor, type of semiconductor (n- or p-type), interface chemistry, processing methodology, presence of defect states and doping concentration of the semiconductor [3–5]. The exposure of Schottky contacts in the radiation environments will lead to considerable variations in their current-voltage (I–V) characteristics due to the influence of accumulated defect states. Generally, the Si-based Schottky contacts or other devices like p-n junction diodes, p-i-n diodes, MOSFETs, MESFETs, JFETs are sensitive to the radiation induced damages which are created by energetic X-rays, gamma rays, electrons, protons and neutrons. These radiations will affect the surface, interface and bulk electronic properties of the semiconductor by generating the various defect states [2,5,6–8].

From the fundamental and technological point of view, it is important to examine the radiation-induced effects on the Schottky contact properties such as Schottky barrier height ( $\Phi_B$ ), ideality factor ( $n$ ) and series resistance ( $R_s$ ) [5,9]. These properties are greatly affected by radiation-induced defect states or interface trap states that occupy energy levels within the band gap ( $E_g$ ) of the semiconductor. These

occupied trap states can behave as donor or acceptor depending on their position with respect to Fermi level ( $E_F$ ). The charge state of the interface trap changes when it crosses the  $E_F$  (i.e., positive above  $E_F$  and negative below  $E_F$ ). When a voltage is applied to the Schottky contact, these interface trap levels move up or down (along with the valence and conduction bands) relative to  $E_F$ , thereby influencing the band bending properties of the Schottky junction or simply the I–V characteristics. It is expected that these effects should be present for Si-Schottky contacts which are exposed to radiation environments [2,5,9].

For various reasons, Al is an important metal in the semiconductor device technology. The Al contacts to Si is uniquely suited as a single-element metallization system as both Schottky contact (for n-type Si, lightly doped) and ohmic contact (for p-type Si and n-type Si, heavily doped) [10]. Although, the Schottky-barrier formation at Al/n-Si interfaces are reported by various researchers [10–13], the effects of radiation on  $\Phi_B$ ,  $n$  and  $R_s$  are not well known. In the last three decades, several irradiation studies on different metal/semiconductor Schottky contact systems were carried out by irradiating with electrons [14,15], neutrons [16,17], protons [18], swift heavy ions [19] and gamma radiations [20,21]. However, the gamma irradiation effects on Al/n-Si Schottky contacts are somewhat limited. In this view, the present article is intended to report on the gamma irradiation effects on n-Si wafer and Al/n-Si Schottky contacts up to an elevated cumulative radiation dose of 1500 kGy. The influence of gamma irradiation dose on the I–V

\* Corresponding author.

E-mail address: [pramod.shetty@manipal.edu](mailto:pramod.shetty@manipal.edu) (P.K. Shetty).

<https://doi.org/10.1016/j.nimb.2018.09.035>

Received 22 June 2018; Received in revised form 22 September 2018; Accepted 24 September 2018

Available online 01 October 2018

0168-583X/ © 2018 Elsevier B.V. All rights reserved.

characteristics of Al/n-Si Schottky contacts is explained in detail by studying both bulk and interface properties using different techniques including X-ray diffraction (XRD), Raman spectroscopy, I–V characteristics and photoelectron spectroscopy. The obtained results are compared with our previous electron beam irradiation studies on Al/n-Si Schottky contacts [5,9].

## 2. Experimental details

The phosphorus doped Si (1 0 0) wafer having thickness of 500  $\mu\text{m}$  and resistivity  $\sim 30 \Omega\text{cm}$  was procured from Sigma Aldrich®, India. The samples were diced into the dimensions of  $5 \times 5$  and  $10 \times 10$  mm. These diced samples were then cleaned according to standard procedures. The cleaning procedure consisted of following steps. First degreasing samples in the acetone and methanol, followed by rinsing in the deionized (DI) water for 5 min. After that, the samples are dipped into 2% diluted HF solution for 2 min to remove the native oxide layer on Si, and then again rinsing in running DI water for 5 min [22]. The Al Schottky contacts are established on cleaned n-Si by using thermal evaporation technique. The deposition is carried out at a rate of  $3 \text{ \AA/s}$ . A base pressure of  $\sim 8 \times 10^{-6}$  mbar was maintained during deposition. The Al thickness was kept at  $\sim 10$  nm with the help of quartz crystal monitor [5].

The gamma irradiation experiment on n-Si wafer and Al/n-Si Schottky contacts were carried out using gamma chamber GC-5000 located at Indira Gandhi Centre for Advanced Research (IGCAR), Kalpakkam India. Gamma chamber GC-5000 has  $^{60}\text{Co}$  pencil sources which are arranged in annular manner around the irradiation volume. The diameter and cylindrical height of the chamber were about 17.2 cm and 20.5 cm respectively. The average gamma photon energy of  $^{60}\text{Co}$  source is 1.25 MeV (as  $^{60}\text{Co}$  source emits gamma photons of two different energies of 1.17 MeV and 1.33 MeV). During the irradiation, the strength of the  $^{60}\text{Co}$  source was approximately 2.8 kGy/hr ( $\sim 78$  rad/s). Both n-Si and Al/n-Si placed in the chamber until a cumulative radiation dose of 500, 1000 and 1500 kGy were delivered on to these samples. The time took for exposing samples to the highest irradiated dose of 1500 kGy was about 535.7 h ( $\sim 22.5$  days).

The XRD studies were carried out using Bruker D8 Advance which is operating at 40 kV and 40 mA (Cu-K $\alpha$ , with  $\lambda = 1.5406 \text{ \AA}$ ) under  $\theta - 2\theta$  geometry condition. The Raman spectra were recorded at room temperature in a back scattering symmetry using a Jobin Yvon Horibra LABRAM-HR visible spectrometer. The spectra were obtained by exciting with 473 nm line of an Ar $^{+}$  laser which was focused on a  $1 \times 1 \mu\text{m}^2$  spot. The laser intensity was kept at approximately 25 mW. The current–voltage (I–V) characteristics of the Al/n-Si Schottky contacts were studied using Keithly 2450 source meter at room temperature (298 K) and under the dark conditions. Copper pressure contacts are used as ohmic contacts during I–V measurements [9]. The XPS studies of n-Si and Al/n-Si Schottky contacts were carried out by using EA-125 Omicron analyzer with Al-K $\alpha$  (1486.6 eV) as a source of x-rays. The effective work function (EWF) measurements of the n-Si and Al surface were performed at 40 eV photon energy using synchrotron radiation (Indus-1 AIPES Beamline-2, RRCAT India) [5].

## 3. Results and discussion

### 3.1. Structural modifications in the n-Si crystal

Fig. 1(a) shows the standard (4 0 0) reflection of Si before and after gamma irradiation at different irradiation doses. The observed variations in the peak position and peak width are not significant except at 500 kGy. The lattice constant ( $a$ ) of Si is evaluated from the (4 0 0) reflection using the relation [23]:

$$a = 2 \cdot \frac{\lambda}{\sin \theta} \quad (1)$$

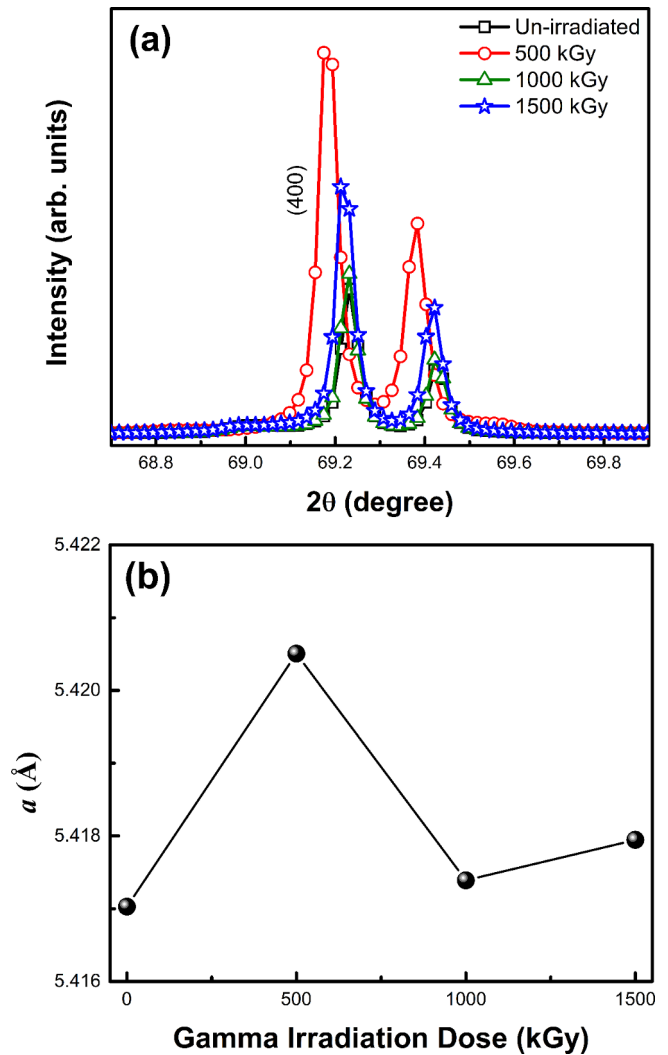


Fig. 1. XRD of n-Si (1 0 0) before and after gamma irradiation at different irradiation doses (a) (4 0 0) peak of Si showing the irradiation induced lattice strain (b) variation of lattice constant  $a$  at different gamma irradiation doses.

where  $\lambda$  is the wavelength of the X-ray used ( $1.5406 \text{ \AA}$ ) and  $\theta$  is the Bragg angle. The modification in  $a$  of n-Si at different gamma irradiation doses is shown in Fig. 1(b). As noticed, the overall modifications in  $a$  are not significant after gamma irradiation. However, its anomalous variations at different irradiation doses are caused due to the presence of gamma induced defect states in the crystal. Since the nature of lattice deformation (contraction or dilation) along the three crystallographic axes usually depends upon the defect states and their concentration [24,25].

Fig. 2 shows the Raman spectra of n-Si before and after gamma irradiation at different irradiation doses. The spectra at different irradiation doses is normalized to the Raman mode of the un-irradiated sample ( $520.9 \text{ cm}^{-1}$ ). To account for the gamma induced modifications in the n-Si crystal, the spectra is further fitted by Lorentzian peak. The fitted spectra along with their peak parameters such as peak position and peak widths are shown in Fig. 2. The overall variation in the peak parameters are not significant after gamma irradiation. However, small variations in their values are indicating the presence of gamma induced defect states in the n-Si crystal. In general, the irradiation induced damage ( $A_{\text{norm}}$ ) is defined as ratio of the peak area of irradiated sample to the peak area of un-irradiated sample. The parameter,  $A_{\text{norm}} < 1$  indicates the degradation in the ordering of atoms in the crystal or the lattice disorder induced by the defect states in the crystal [26,27]. At

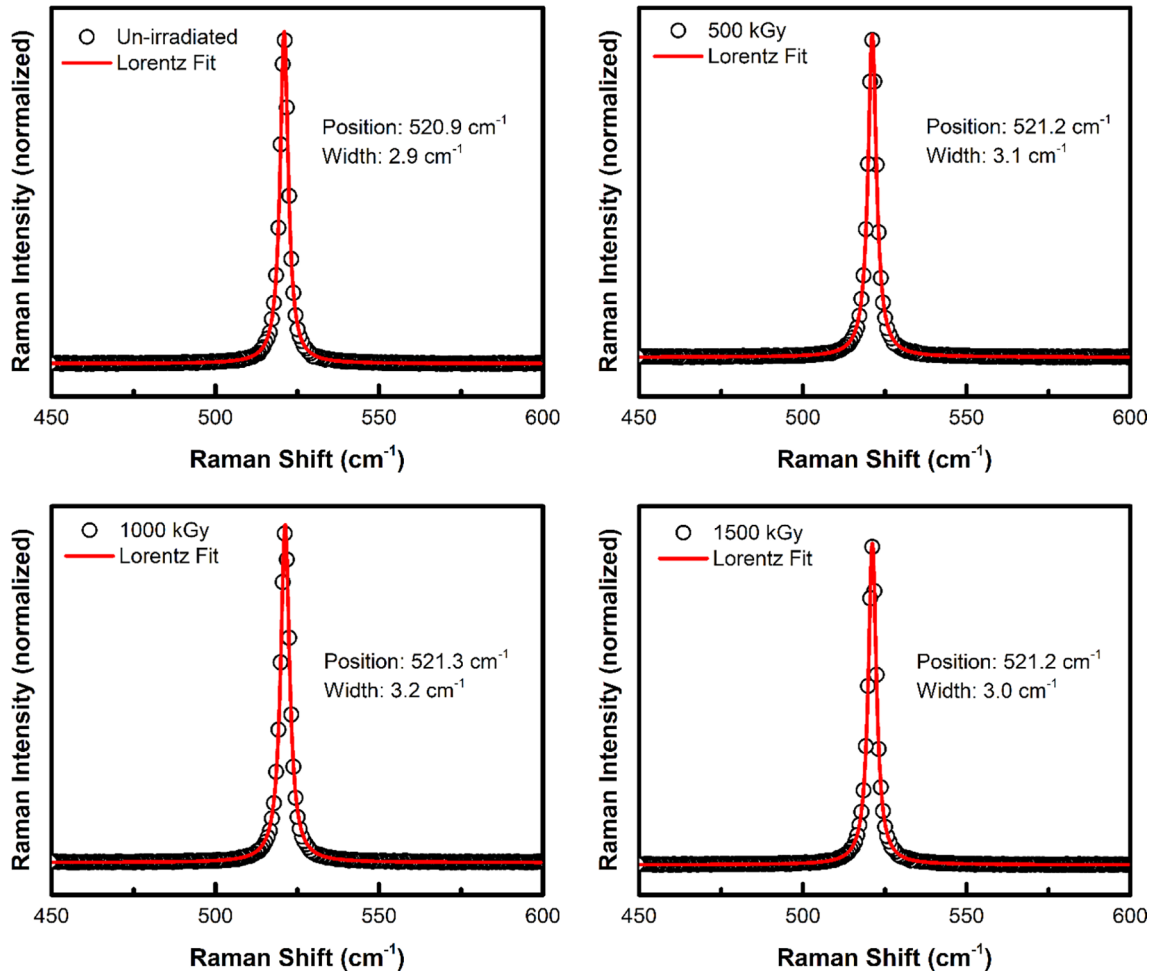


Fig. 2. Raman spectra of n-Si before and after gamma irradiation at 500, 1000 and 1500 kGy irradiation doses. The peak parameters given in spectra are obtained by fitting Lorentzian peak profile.

500 kGy irradiation dose, the evaluated  $A_{\text{norm}}$  is 0.84 which is less than unity while at 1000 kGy and 1500 kGy the  $A_{\text{norm}}$  values are found to be nearly equal to unity (1.1 and 1.04). This indicates that the gamma induced lattice disorder due to defect accumulation is greater at 500 kGy. But as the dose is increased to 1000 kGy and 1500 kGy, a partial recovery of the damaged lattice is noticed. Similar results are evident from Fig. 1, where the modification in  $a$  at 1000 kGy and 1500 kGy are not significant compared to the un-irradiated one. Thus, from the XRD and Raman spectroscopy analysis, it can be concluded that the crystalline nature of n-Si is not greatly affected due to the presence of gamma induced defect states.

### 3.2. Analysis of I–V characteristics

Fig. 3 shows the I–V characteristics of Al/n-Si Schottky junctions before and after gamma irradiation. Clearly the modifications in the I–V characteristics are observed at different gamma irradiation doses. It is common that the gamma radiations (ionizing radiations) cause excess forward current and reverse current (leakage current ( $I_L$ ), Table 1) due to the build-up of positive space charge in the interfacial oxide, increase in the surface recombination velocity and carrier removal processes [2]. Therefore, the increase of  $I_L$  in the present case are ascribed to gamma induced defect states in the interface as well as bulk of the n-Si crystal via ionization and displacement damage mechanisms [2,5]. The modification in these I–V characteristics at different gamma irradiation doses can be explained by applying thermionic-emission (TE) model of

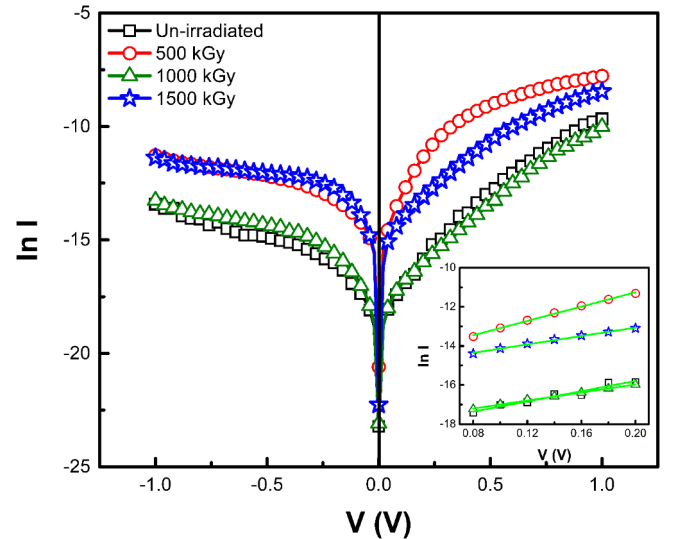


Fig. 3. Semi-log plot of the Al/n-Si Schottky contacts before and after gamma irradiation at different irradiation doses. Insert shows the linear region where the thermionic-emission (TE) model is applied to determine ideality factor ( $n$ ) and Schottky barrier height ( $\Phi_B$ ).

Schottky junctions. According to which, the expression for the variation in the forward current  $I$  for the applied voltage  $V$  across a Schottky junction is related by [1]

**Table 1**

Al/n-Si Schottky contact parameters before and after gamma irradiation evaluated by applying thermionic emission (TE) model and Cheung model.

Sample	TE Model			Cheung Model			$I_L(\mu\text{A})$ at – 500 mV
	n	$\Phi_B(\text{eV})$	$I_s(\text{nA})$	n	$\Phi_B(\text{eV})$	$R_s(\text{k}\Omega)^*$	
Un-irradiated	2.98	0.80	10.21	4.63	0.76	2.85	0.33
500 kGy	2.13	0.71	334.71	1.67	0.72	2.42	5.10
1000 kGy	3.80	0.79	14.92	4.32	0.78	2.53	0.58
1500 kGy	3.63	0.72	247.96	3.66	0.71	5.04	5.67

\* Determined from  $H(I)$  vs.  $I$  plot.

$$I = I_s \left[ \exp\left(\frac{qV}{nkT}\right) - 1 \right] \quad (2)$$

where

$$I_s = AA^*T^2 \exp\left(-\frac{q\Phi_B}{kT}\right) \quad (4)$$

is the reverse saturation current,  $A$  is effective area of the Schottky contact ( $3.14 \times 10^{-4} \text{ cm}^2$ ),  $A^*$  is the Richardson constant (for n-Si,  $A^* = 112 \text{ A.cm}^{-2} \text{ K}^{-2}$  [3,9]),  $q$  is charge of the electron,  $\Phi_B$  is Schottky barrier height,  $k$  is Boltzmann constant and  $T$  is absolute temperature. The parameter  $n$  in Eq. (2) is known as ideality factor which accounts for non-ideal behavior of the Schottky contact [1,3]. For  $V > 3kT/q$ , the term  $-I_s$  in Eq. (2) can be neglected. We then obtain a simplified straight line equation of the form:

$$\ln I = \frac{qV}{nkT} + \ln I_s \quad (5)$$

Therefore by plotting  $\ln I$  vs.  $V$ , the parameters  $\Phi_B$  and  $n$  can be determined from the intercept and slope respectively. As seen from Eq. (5), the  $\ln I$  vs.  $V$  plot (Fig. 3) should be linear. However, most of the practical Schottky contacts will exhibit deviation from the linearity behavior at higher voltages. In the present case, the deviation is observed for  $V > 0.2 \text{ V}$ . This type of behavior is attributed to the factors such as the presence of thin insulating layer (oxide layer) at the interface, presence of interface trap states (whether processed and/or radiation-induced) and defects states in the n-Si crystal [5,9,15]. The insert in the Fig. 3 shows the linear voltage region in the range of  $0.08\text{--}0.2 \text{ V}$ . In this voltage region, TE model is applied and the parameters  $\Phi_B$  and  $n$  are extracted by using Eqs. (4) and (5). The obtained values are reported in Table 1.

However, the contact parameters  $n$  and  $\Phi_B$  which are determined by applying TE model does not take into account of series resistance ( $R_s$ ) across the junction. The effect of  $R_s$  is modelled as a series combination of a diode and a resistor with resistance  $R_s$  through which the current  $I$  flows. Therefore, to account for the role of  $R_s$  on  $n$  and  $\Phi_B$ , the term  $V$  in TE model Eq. (2), should be replaced by  $(V - IR_s)$ . Therefore, for  $V > 3kT/q$ , the modified TE model Eq. (2) in consideration of  $R_s$  has the form [5,9,28]

$$I = I_s \left[ \exp\left(\frac{q(V - IR_s)}{nkT}\right) \right] \quad (6)$$

The differentiation of Eq. (6) with respect to  $I$  leads to the simplified form as,

$$\frac{dV}{d(\ln I)} = R_s I + \frac{nkT}{q} \quad (7)$$

By plotting  $\frac{dV}{d(\ln I)}$  vs.  $I$ , the  $R_s$  and  $n$  can be determined from the slope and intercept respectively. Similarly, upon substituting for  $I_s$  from Eq. (5) into Eq. (6), we arrive at the simplified expression of the form:

$$H(I) = R_s I + n\Phi_B \quad (8)$$

with

$$H(I) = V - \frac{nkT}{q} \ln\left(\frac{I}{AA^*T^2}\right) \quad (9)$$

Therefore the slope and intercept of the  $H(I)$  vs.  $I$  plot gives  $R_s$  and  $\Phi_B$  respectively. Here, the  $n$  value obtained from Eq. (7) must be considered in the evaluation of  $\Phi_B$ . Also, the downward curvature of the linear  $I$ - $V$  plot must be selected in the evaluation methodology. The Eqs. (7) and (8) are derived by Cheung and Cheung and are referred as graphical Cheung functions or simply Cheung model [28]. The Cheung plots  $\frac{dV}{d(\ln I)}$  vs.  $I$  and  $H(I)$  vs.  $I$  which are fitted by straight lines are shown in Fig. 5 and the obtained values of  $n$ ,  $\Phi_B$  and  $R_s$  values are reported in Table 1.

As noticed, for all the cases  $n$  is greater than unity. This indicates the non-ideal or inhomogeneous nature of the Schottky junction [3,4]. In the present case of Al/n-Si Schottky junction, the inhomogeneity is attributed for the lattice mismatch between Al and Si, less thickness of Al and presence of defects states (processed and radiation-induced) in the interface as well as bulk of the n-Si crystal [5,9,11–13]. The discrepancies between TE model and Cheung model values are caused due to the effect of  $R_s$  and role of interface trap states. The variations in the  $n$  and  $\Phi_B$  after gamma irradiation are attributed to the combined influence of small increase in  $a$  of the Si crystal (Fig. 1) and the presence of gamma-induced defect states in the interface of Al/n-Si junction as well as bulk of the n-Si crystal. These irradiation modifications are usually expected to occur via the fundamental ionization and displacement damage mechanisms [2,5–7,9].

### 3.3. Power law characteristics

Due to barrier inhomogeneity ( $n > 1$ ) and high value of  $R_s$ , the Al/n-Si contacts are not showing ideal  $I$ - $V$  characteristics of the form of Eq. (5). This clearly indicates the participation of different transport mechanisms other than thermionic emission of electrons over the barrier  $\Phi_B$  of the Schottky junction. In order to realize the dominant transport mechanism across the Schottky junction, one can plot the power law characteristics. It states that:  $J \propto V^m$  where  $J$  is the current density,  $V$  is the applied voltage and  $m$  is the power [29]. Here the power  $m$  indicates the dominant transport mechanism across the junction. The power  $m \approx 1$  and  $m > 2$  are attributed for thermionic emission of electrons and space-charge limited emission or space-charge limited conduction (SCLC) conduction processes. Fig. 5 shows the power law characteristics of Al/n-Si Schottky contacts before and after gamma irradiation. The characteristics are approximately divided into two voltage regions (Region I and Region II). Each region represents a dominant type of transport mechanism [5,29]. In the lower bias voltage or Region I, the  $m$  (slope) values were found to be approximately unity. The dominant transport mechanism in this region is therefore the thermionic emission of electrons over Schottky barrier  $\Phi_B$ . But in the Region II, the current density  $J$  is found to vary with a certain degree  $m$  (slope) of the voltage ( $V$ ). The obtained  $m$  values in the Region II are found to be greater than 2. This indicates the activation of interface trap states in the conduction mechanism. Therefore, the dominant transport mechanism in the Region II must be the SCLC process. In the present case, the interface trap states are the Si–O bonds and Al–O bonds. Usually they are amphoteric in nature [30]. Therefore, these trap states can act either as acceptor or donor states depending on their position with respect to Fermi level ( $E_F$ ) [2,5,29]. In addition to TE and SCLC mechanisms,  $n > 2$  indicates that small contribution from tunneling and tunneling through trap-states are also expected to take place throughout the voltage region [3,4,31].

Most of the irradiation studies show a regular trend either increase or decrease in some of the parameters. But in the present case no such trends were obtained (Figs. 1–4 and Table 1). This could be due to the smaller thickness of Al contact and the nature of defect states which are present in the interface as well as bulk of n-Si. However, a particular trend is observed among the determined parameters. In short an inverse



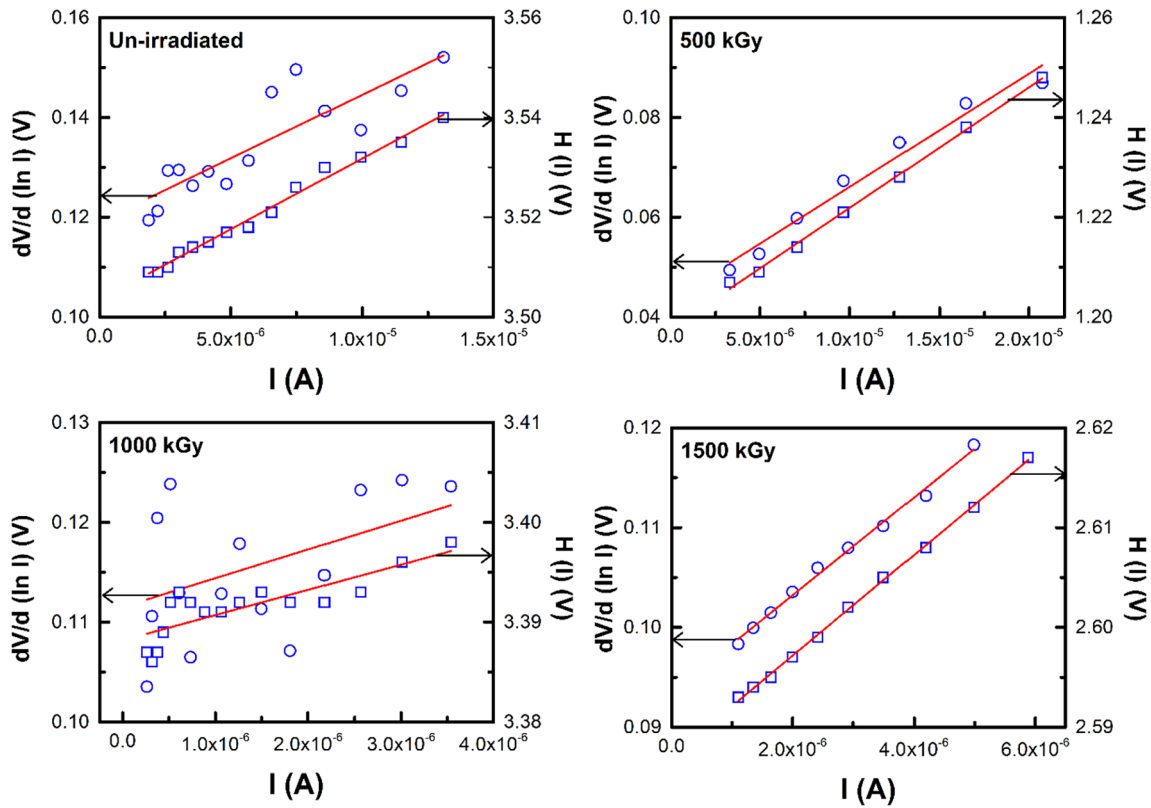


Fig. 4. Cheung plots of Al/n-Si Schottky contacts before and after gamma irradiation at different irradiation doses.

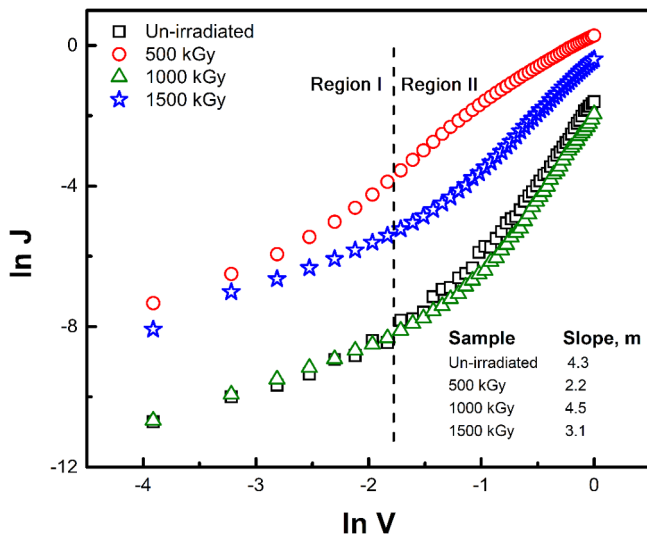


Fig. 5. Power law characteristics of Al/n-Si Schottky contacts before and after gamma irradiation.

relationship between the  $\alpha$  of n-Si and junction parameters ( $n$ ,  $\Phi_B$ , and  $m$ ) of Al/n-Si contacts is observed for different irradiation doses. This implies the role of defect states and small lattice strain that are affecting the Al/n-Si junction properties.

### 3.4. Photoelectron spectra analysis

Fig. 6(a) shows the core Al 2p XPS spectra of the irradiated Al/n-Si Schottky contact. The Gaussian decomposition showed Al metallic binding energy state at 73.1 eV, the  $\text{Al}_2\text{O}_3$  or  $\text{Al}/\text{AlO}_x$  binding energy state at 75.2 eV and a gamma induced chemical state at  $\sim 77.0$  eV. This chemical state could be caused due to the interaction of the diffused Al

atoms with  $\text{SiO}_x$  states in the interface. This causes the formation of non-uniform  $\text{AlO}_x$ – $\text{SiO}_x$  (or  $\text{Al}_2\text{O}_3$ – $\text{SiO}_2$ ) medium at the interface of Al/n-Si Schottky junction. These Al–O or Si–O bonds would act as interface trap states and contribute greatly to the band bending properties and different conduction mechanisms. Similar results were also found in the electron beam irradiated Al/n-Si Schottky contacts [5].

Fig. 6(b) shows valence band spectra of Al/n-Si Schottky contact surface which is taken at 40.0 eV photon energy using synchrotron radiation. The distortions observed in the spectra are caused due to the Al oxidation and the generation of trap states involving the oxidized chemical species of Al and Si [5]. The insert given in the plot shows the secondary energy cut-off (SECO) region of the spectra. The intersection point as shown by the horizontal and vertical line is equal to binding energy at the SECO ( $E_{B0}$ ). Subtracting  $E_{B0}$  from the given excitation photon energy (40.0 eV) gives the effective work function (EWF) of Al [32]. The EWFs of Al were found to be 4.3 eV [5] and 4.8 eV before and after gamma irradiation respectively. This increase in the EWF of Al, along with the modified interface chemistry i.e., interface trap states (Figs. 6 and 7(a)) and a small increase in the lattice parameter  $a$  of the n-Si (Fig. 1) will together influence the band line-up properties at the junction of Al/n-Si Schottky contact.

The schematic representation of the equilibrium energy band diagram of the irradiated Al/n-Si Schottky contact is shown in Fig. 7. The in-depth analysis of the Al/n-Si energy band diagram is detailed in Ref. [5]. At equilibrium,  $E_F$  of n-Si and Al are aligned. The deformation of the n-Si bands ( $V_{bi}$ ) and the barrier which is set up at the metal side known as Schottky barrier ( $\Phi_B$ ). Both the barriers prevent the further diffusion of the charge carriers on either side of the junction. This results in zero net current density at equilibrium. Both  $V_{bi}$  and  $\Phi_B$  sensitive to the presence of different chemical states (interface trap states) at the interface and defect states in the bulk n-Si. The radiation-induced interface trap states or defect states occupies the energy levels within the  $E_g$  of n-Si. These states can behave as donors or acceptors depending on their position with respect to Fermi level ( $E_F$ ). The charge state of

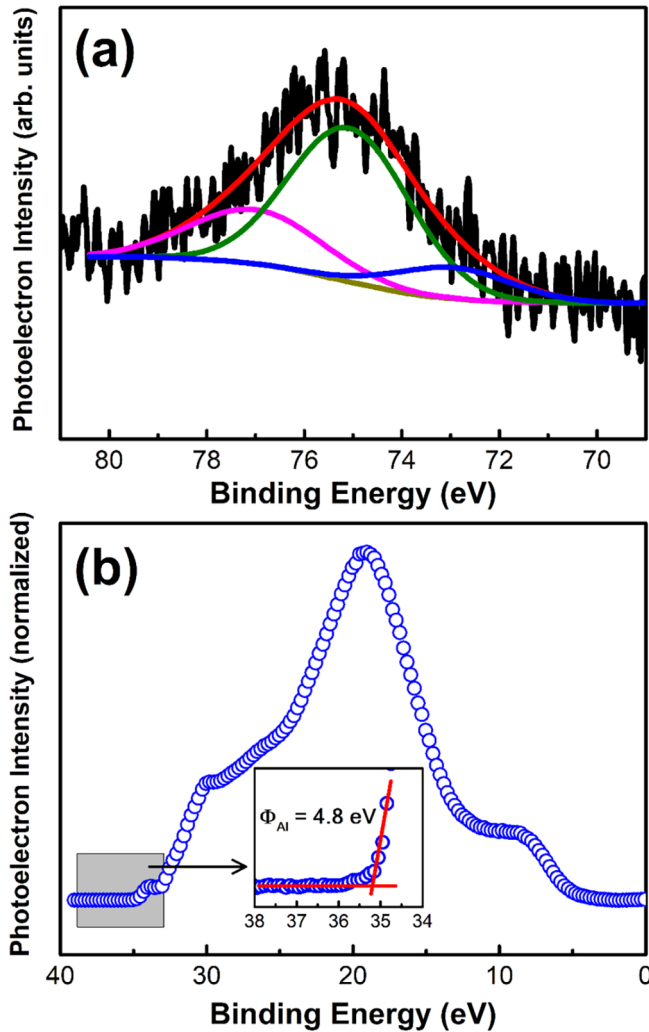


Fig. 6. Photoelectron spectra of gamma irradiated Al/n-Si (a) core Al 2p XPS spectra (b) valence band spectra, inset shows the enlarged secondary energy cut-off region.

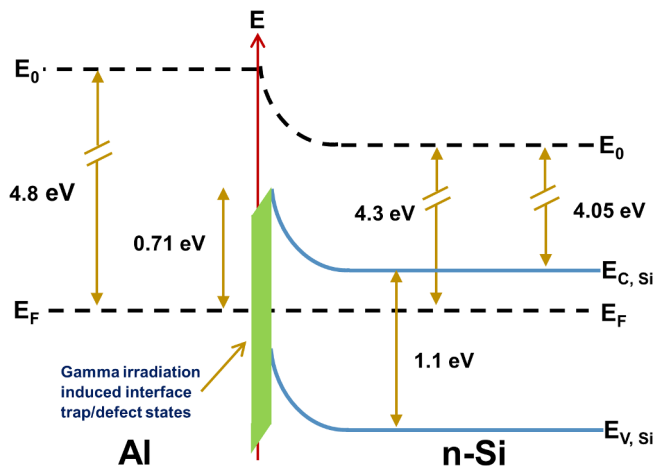


Fig. 7. Energy band diagram of Al/n-Si Schottky junction after gamma irradiation- showing the influence of irradiation induced interface trap states at the interface on the band bending properties ( $E_0$  is the vacuum level,  $E_F$  the Fermi level,  $E_{V,Si}$  is the valence band edge of Si, and  $E_{C,Si}$  is the conduction band edge n-Si).

the gamma induced interface trap changes when it crosses  $E_F$ . In other words, the donor interface trap is neutral when it is below  $E_F$  and becomes positive by donating an electron when it moves above  $E_F$ . Similarly, an acceptor interface trap is in a neutral charge state when it is above  $E_F$  and becomes negative by accepting an electron when it moves below  $E_F$ . Therefore, the precise energy position of  $E_F$  within  $E_g$  of n-Si and  $\Phi_B$  of Al/n-Si depends on the distribution of interface states ( $m$ ) and defect states at a particular irradiation dose. When the voltage  $V$  is applied across the Al/n-Si Schottky junction, gamma-induced interface trap levels (Al-O or Si-O) move up or down (along with the valence and conduction bands) relative to  $E_F$ . Thus, overall affecting the I-V characteristics [2–5].

#### 4. Conclusion

The n-Si and Al/n-Si Schottky contacts were subjected to gamma irradiation at 500, 1000 and 1500 kGy doses. The XRD and Raman spectra analysis showed that the crystalline properties of n-Si are not greatly affected due to gamma induced defect states. However, the I-V characteristics of Al/n-Si Schottky junctions and its parameters  $\Phi_B$ ,  $n$  and  $R_s$  were considerably affected due to presence of gamma induced defect states in the interface as well as in the bulk. The power law characteristics revealed the participation of different competing transport mechanisms including the thermionic emission of electrons, SCLC, tunneling and tunneling through the trap states across the Al/n-Si junction. The XPS studies showed that the oxidized chemical species of Al and Si ( $AlO_x$ – $SiO_x$ ) at the interface were found to act as interface trap states. The increase in the effective work function of Al, amphoteric nature of interface trap states and small lattice strain induced in the n-Si crystal have contributed to the modification in the band bending properties of the Al/n-Si Schottky junction and their I-V characteristics. Therefore, from this study it is concluded that the gamma irradiation up to 1500 kGy dose brings noticeable modification in the surface and interface properties of the Al/n-Si Schottky junction.

#### Acknowledgements

This work has been carried out under UGC DAE CSR Indore, India collaborative research scheme (CSR-IC-BL-48/CRS-145-2014-15/1241). The authors would like to acknowledge M. T. Jose, Hari Krishnan and Shailesh Joshi, RSD, IGCAR India, for providing and carrying out Gamma irradiation process. The authors would like to acknowledge Avinash Wadikar and Sharad Karwal in carrying out PES measurements. The authors are grateful to Vision Group on Science and Technology, Govt. of Karnataka India for instrument facility provided through KFIST grant (VGST/K-FIST (L1) (2014-15)/2015-16 GRD – 377).

#### References

- [1] S.M. Sze, Physics of Semiconductor Devices, second ed., Wiley, New York, 1981.
- [2] P.S.W.P.J. McWhorter, Donor acceptor nature of radiation-induced interface traps, IEEE Trans. Nucl. Sci. 35 (1988) 1154–1159.
- [3] R.T. Tung, Recent advances in Schottky barrier concepts, Mater. Sci. Eng. R Reports 35 (2001) 1–138.
- [4] L.J. Brillson, Contacts for Compound Semiconductors: Schottky Barrier Type, Reference Module in Materials Science and Materials Engineering (2016) 1–8. doi: 10.1016/B978-0-12-803581-8.01788-4.
- [5] I.P. Vali, P.K. Shetty, M.G. Mahesha, V.C. Petwal, J. Dwivedi, D.M. Phase, R.J. Choudhary, Implications of electron beam irradiation on Al/n-Si Schottky junction properties, Microelectron. Reliab. (2018), <https://doi.org/10.1016/j.microrel.2018.07.031>.
- [6] P.J. Drevinsky, A.R. Frederickson, D.W. Elsaesser, Radiation-induced defect introduction rates in semiconductors, IEEE Trans. Nucl. Sci. 41 (1994) 1913–1923.
- [7] G. Lutz, Semiconductor and Electronic Devices, Springer, 1999.
- [8] Shailesh K. Khamari, V.K. Dixit, S. Tapas Ganguli, S.D. Singh Porwal, R.K. Sanjay Kher, S.M. Oak Sharma, Effect of 60Co  $\gamma$ -ray irradiation on electrical properties of GaAs epilayer and GaAs p-i-n diode, Nucl. Instrum. Methods Phys. Res. B 269 (2011) 272–276.
- [9] I.P. Vali, P.K. Shetty, M.G. Mahesha, V.C. Petwal, J. Dwivedi, R.J. Choudhary,

- Tuning of Schottky barrier height of Al/n-Si by electron beam irradiation, *Appl. Surf. Sci.* 407 (2017) 171–176.
- [10] C. Howard, Card, aluminum-silicon schottky barriers and ohmic contacts in integrated circuits, *IEEE Trans. Electron Devices* 23 (1976) 538–544.
- [11] Y. Miura, K. Hirose, K. Aizawa, N. Ikarashi, H. Okabayashi, Schottky barrier inhomogeneity caused by grain boundaries in epitaxial Al film formed on Si (111), *Appl. Phys. Lett.* 61 (1992) 1057.
- [12] M. Siad, A. Keffous, S. Mamma, Y. Belkacem, H. Menari, Correlation between series resistance and parameters of Al/n-Si and Al/p-Si Schottky barrier diodes, *Appl. Surf. Sci.* 236 (2004) 366–376.
- [13] Hai-feng Zhang, Arunodoy Saha, Wen-cheng Sun, Meng Tao, Characterisation of Al/Si junctions on Si (100) wafers with chemical vapor deposition-based sulfur passivation, *Appl. Phys. A* 116 (2014) 2031–2038.
- [14] Sheeja Krishnan, Ganesh Sanjeev, Manjunatha Pattabi, Electron irradiation effects on the Schottky diode characteristics of p-Si, *Nucl. Instrum. Methods Phys. Res. B* 266 (2008) 621–624, <https://doi.org/10.1016/j.nimb.2007.11.049>.
- [15] E. Omotoso, W.E. Meyer, F.D. Aurret, A.T. Paradzah, M. Diale, S.M.M. Coelho, P.J. Janse van Rensburg, The influence of high energy electron irradiation on the Schottky barrier height and the Richardson constant of Ni/4H-SiC Schottky diodes, *Mater. Sci. Semicond. Process.* 39 (2015) 112–118, <https://doi.org/10.1016/j.mssp.2015.04.031>.
- [16] Zhang Lin, Zhang Yimen, Zhang Yuming, Han Chao, Neutron radiation effect on 4H-SiC MESFETs and SBDs, *J. Semicond.* 31 (114006) (2010) 1–4, <https://doi.org/10.1088/1674-4926/31/11/114006>.
- [17] F. Nava, A. Castaldini, A. Cavallini, P. Errani, V. Cindro, Radiation detection properties of 4H-SiC Schottky diodes irradiated Up to  $10^{16}$  n/cm<sup>2</sup> by 1 MeV neutrons, *IEEE Trans. Nucl. Sci.* 53 (2006) 2977–2982, <https://doi.org/10.1109/TNS.2006.882777>.
- [18] A.M. Ivanov, N.B. Strokan, V.V. Kozlovski, A.A. Lebedev, Effect of electron and proton irradiation on characteristics of SiC surface-barrier detectors of nuclear radiation, *Semiconductors* 42 (2008) 363–369, <https://doi.org/10.1007/s11453-008-3023-4>.
- [19] S. Kumar, D. Kanjilal, Barrier, height modification of Au/n-Si Schottky structures by swift heavy ion irradiation, *Nucl. Instrum. Methods Phys. Res. B* 248 (2006) 109–112.
- [20] Ş. Karataş, A. Türit, Ş. Altındal, Effects of 60Co  $\gamma$ -ray irradiation on the electrical characteristics of Au/n-GaAs (MS) structures, *Nucl. Instrum. Methods Phys. Res. A* 555 (2005) 260–265.
- [21] A. Tataroğlu, Ş. Altındal, M.M. Bülbül, 60Co  $\gamma$  irradiation effects on the current-voltage (I-V) characteristics of Al/SiO<sub>2</sub>/p-Si (MIS) Schottky diodes, *Nucl. Instrum. Methods Phys. Res. Sect. A* 568 (2006) 863–868.
- [22] Jingyan Zhang, William R. Harrell, Analysis of I-V characteristics of Al/4H-SiC Schottky diodes, *J. Vac. Sci. Technol. B* 21 (2003) 872–878.
- [23] Suryanarayana, M. Grant Norton, X-Ray Diffraction A Practical Approach, Springer, 1998.
- [24] Leonid V. Azaroff, Introduction to Solids, Mc-Graw Hill, 1960.
- [25] A.N. Prabhu, Pramoda Kumara Shetty, Indudhar Panduranga Vali, Hemanth Kumar, Sowmyasree Udupa, Gamma and neutron irradiation effects on the structural and optical properties of potash alum crystals, *Nucl. Instrum. Methods Phys. Res. B* 413 (2017) 37–41.
- [26] R. Menzel, K. Gärtner, W. Wesch, H. Hobert, *J. Appl. Phys.* 88 (2000) 5658.
- [27] R. Héliou, J.L. Brebner, S. Roorda, *Nucl. Instrum. Methods Phys. Res. B* 175 (2001) 268.
- [28] S.K. Cheung, N.W. Cheung, Extraction of Schottky diode parameters from forward current-voltage characteristics, *Appl. Phys. Lett.* 49 (1986) 85–87.
- [29] F. Yakuphanoglu, N. Tugluoglu, S. Karadeniz, Space charge-limited conduction in Ag/p-Si Schottky diode, *Phys. B Condens. Matter.* 392 (2007) 188–191.
- [30] Y.C. Du, H. Wang, B.Z. Li, D.C. Sun, Z.Q. Yu, F.M. Li, Rapid formation of ultra-thin dielectrics by Si surface modification using large area low energy electron beam, *Vacuum* 41 (1990) 796–799.
- [31] M. Tuominen, Trap-assisted tunneling in high permittivity gate dielectric stacks, *J. Appl. Phys.* 87 (2000) 8615.
- [32] R. Schlaf, H. Murata, Z.H. Kafafi, Work function measurements on indium tin oxide films, *J. Electron. Spectrosc. Relat. Phenom.* 120 (2001) 149–154.